![BCHD logo]

Computational study of antiviral, anti-bacterial, and anticancer activity of green-extracted Sidr (Ziziphus spina-Christi) fruit phenolics

Fadwa W. Abdulqahar[1], Zuhair I. Mahdi[2], Shaymaa H. M. Al-kubaisy[3], Feryal F. Hussein[4], Malikakhon Kurbonova [5], Marwa M. El-Said[6] and Tamer M. El-Messery[5*]

[1]Department of Food Science, College of Agriculture, University of Anbar, Anbar, Ramadi City, Ministry of Higher education and Scientific Research, Iraq; [2]Central Public Health Laboratory, Anbar Health Directorate, Anbar, Ramadi City, Ministry of Health, Iraq; [3]College of Pharmacology, University of Anbar, Anbar, Ramadi City, Ministry of Higher education and Scientific Research, Iraq; [4]Dept. or Food Science, College of Agriculture, Tikrit University, Ministry of Scientific research and Higher Education, Tikrit, Saladin Province, Iraq; [5]International Research Centre "Biotechnologies of the Third Millennium", Faculty of Biotechnologies (BioTech), ITMO University, St. Petersburg, 191002, Russia; [6]Dairy Department, National Research Centre, Cairo, 12622, Egypt

*Corresponding Author: Tamer M. El-Messery: International Research Centre "Biotechnologies of the Third Millennium", Faculty of Biotechnologies (BioTech), ITMO University, St. Petersburg, 191002, Russia

ABSTRACT

Background: Hepatitis may result in inflammation, swelling, cirrhosis, cancer, and failure. Food-born bacteria like *Escherichia coli*, *Staphylococcus aureus*, *Vibrio cholera*, and *Helicobacter pylori* have widely developed antibiotic resistance in recent years. The latter is a common hazardous pathogen that may lead to stomach vacuoles and gastric cancer. Despite the toxicity, medication resistance, and/ or financial burdens of conventional cancer medicines, most breast cancer patients globally develop recurrence or relapse distant metastases in many other organs after receiving initial common treatment. Such cases need to find solutions that differ from conventional medicines. Plants are an essential source of efficient bioactive compounds that could be utilized in fighting bacterial and viral infections and/or cancer safely. Due to their capability to control many molecular pathways with less harmful effects, the phytochemicals used in complementary medicine have recently attracted more attention. Most of these phytochemicals are members of one of the alkaloids, phenolics, carotenoids, flavonoids, and/ or terpenoids groups. Sidr (*Ziziphus spina-Christi* (L.) Willd) is a well-known, traditionally used fruit for curing many diseases in the Middle East. Network medicine and AI technologies can rapidly hasten the discovery of new drug alternatives.

Objective: This study aimed to extract phenolic compounds from Sidr via two green chemistry approaches, then to predict the anticancer and the antimicrobial effect of the characterized phytochemicals towards certain microorganisms.

Methods: **Sidr fruit powder was extracted via supercritical CO$_2$ and ethanol as co-solvent and the defatted residues were extracted via the hydro-ethanolic ultrasound assisted extraction to obtain a higher yield of phenolic compounds.** The phenolic compounds were characterized and computationally studied for their biological activity against different protein targets of hepatitis virus, food- and water-borne pathogenic bacteria, and breast cancer via Molecular docking and Molecular Dynamics. Additionally, ADMET study was performed for the compounds with high Vina score and good dynamics results.

Results: Chemical analysis revealed the presence of seven different phenolic compounds (Gallic acid, caffeic acid, Pyrocatechol, Coumaric acid, Ferulic acid, Quercetin, and Cinnamic acid). By the results obtained from molecular docking phytochemical Quercetin showed good binding scores and interactions with *S. aureus* tyrosyl-tRNA synthetase (1JIJ), *V. cholera* UDP-N-acetylenolpyruvoylglucosamine reductase (3I99), Human topoisomerase Ⅱ beta (3QX3) and *H. pylori* shikimate kinase (3N2E) with Vina scores equal -9.9, -9.4, -9.3 and -8.5 respectively. ADMET analysis showed that Quercetin obeyed Lipinski's rule and had high GI absorbance, no BBB, and low toxicity within limits. Molecular dynamics studies revealed that *V. cholera* (3I99), Human topoisomerase Ⅱ beta (3QX3), and *H. pylori* shikimate kinase (3N2E) proteins don't show effective stabilities, and more fluctuations were observed. Quercetin with *S. aureus* tyrosyl-tRNA synthetase (1JIJ) showed good stability and formed a stable complex with good RMSD and RMSF.

Conclusion: Based on the results obtained, the compound Quercetin can be a potent molecule to treat bacterial infections related to the antibiotic-resistant *Staphylococcus aureus*. Sidr (*Ziziphus spina-Christi* (L.) Willd) is a widely consumed fruit worldwide and it has been used in traditional medicine since ancient times, so using this plant's extracts may be a potent anti-bacterial treatment. These results need further in vitro and in vivo studies in the future to prove their accuracy.
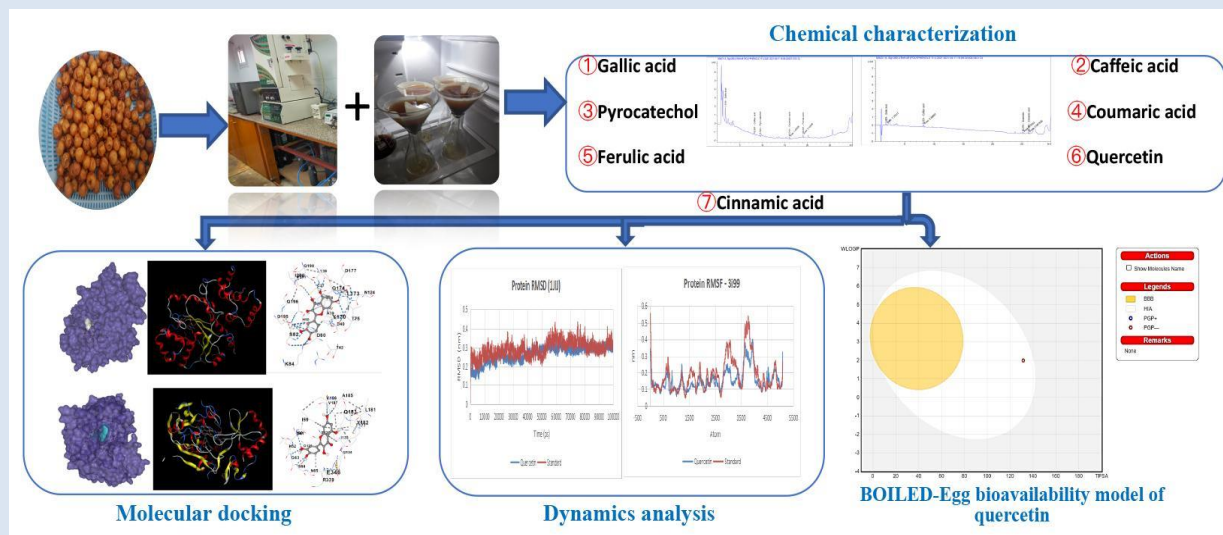
INTRODUCTION

Hepatitis results in liver infection, which then causes inflammation and liver swelling [1]. HBV causes chronic liver diseases like cirrhosis, cancer, and failure [2]. Even though there are some licensed medications and genetically modified vaccines against the hepatitis B virus (HBV), HBV infection remains a serious public health issue worldwide. Even interferon-alpha and nucleoside analogs, which are approved medicinal medications, have their limitations. Medications or other treatments cannot cure hepatitis B [3]. There are about 185 million HCV-infected people worldwide, and no effective drug exists [4].

Food-born bacteria like *Escherichia coli*, *Staphylococcus aureus*, and *Vibrio cholera* have widely developed antibiotic resistance in recent years [5-6]. *Helicobacter pylori* is a common pathogen most typically spread by contact with contaminated saliva, vomit or stool, but can also be spread through food. Some strains of H. pylori cause gastric malignant tumors and severe gastroduodenal diseases. Some can cause the stomach host cells to develop vacuoles by inducing holes [7].

The most prevalent cancer in the world is breast cancer. After receiving initial conventional treatment, 20%–30% of individuals with early breast cancer develop recurrence or relapse with distant metastases, such as bone, lung, liver, and/or brain metastases. Since metastatic breast cancer (MBC) is incurable, distant metastases account for most breast cancer-related deaths. Future treatment paradigms for breast cancer aim to personalize care and de-escalate and escalate treatment based on tumor biology and early therapy response. Equal access to therapeutic advances worldwide continues to be the biggest issue facing breast cancer therapy globally after novel therapy developments [8-9]. Conventional cancer medicines have been fraught with difficulties, such as toxicity, medication resistance, and financial burdens.

However, due to their capacity to control a variety of molecular pathways with a less harmful effect, phytochemicals used in complementary alternative medicine (CAM) have recently attracted more attention [10]. Alternatively, plants are an essential source of efficient bioactive compounds that could safely fight bacterial and viral infections and/or cancer. Some of the most thoroughly studied plant compounds have antitumor activity, including alkaloids, carotenoids, flavonoids, and phenolics [11].

Phytopharmaceuticals and phyto nutraceuticals are substances with pharmacological properties that are obtained from plants. They constitute a significant proportion of pharmaceuticals derived from plant-based compounds instead of synthetics. Fruits, vegetables, herbs, and/or supplements derived from them are all examples of acquiring phytopharmaceuticals. They are crucial to the preservation of healthy bodily processes. Phytopharmaceuticals primarily focus on particular receptors, obstructing illness processes and pathogenic organisms' life cycles [12].

Ziziphus spina-Christi (L.) Willd. (Sidr or Nabk as called in Arab countries), it is a widely distributed plant in the Middle East region. It is identified as a "holy" plant from an ethnic point of view for different religions, such as Muslim, Jewish, and Christian [13]. Sidr is well known as traditional medicine in the middle east region for its therapeutic properties like sedative, anti-inflammatory, anti-swelling, anti-constipation, antiaging, and anti-insomnia effects [14-15]. Most Ziziphus plant species are non-toxic to humans. Numerous investigations on the Ziziphus species have revealed that the roots, leaves, and fruits give them medicinal qualities [16]. Sidr is a sweet, pleasant fruit that contains many antioxidants and therapeutic bioactive compounds like polyphenols,

flavonoids, saponins, and vitamins [17]. It is used directly as fresh fruit in its harvesting season, spring, or dried and frequently serves to meet the local population's dietary and nutritional needs in some developing countries [18].

Green extraction techniques are preferred over traditional methods due to their low cost, environmental friendliness, speed, and performance efficiency. Supercritical CO_2 and ultrasonic-assisted extraction techniques are the most influential and frequently utilized methods in extracting bioactive compounds from plant origin. These techniques eliminate the degradation of thermally sensitive compounds and the poisonous effects of using solvents. Whether it's the health impact due to solvent traces remaining in the extract, making them unsafe for consumption in food or drugs, or the impact on the ecosystem [19]. Network medicine and AI technologies that are rapidly evolving, potent, and innovative can hasten the discovery of new treatments and drug alternatives [20]. While the computational drug-alternatives discovery techniques use structural data of both the drug target and the chemical compound, chemical biology clarifies the biological functions of targets [21-22].

This study aimed to identify the phenolic compounds extracted by different green extraction methods and predict their probable therapeutic effects as antiviral, antibacterial, and anticancer drug-alternative agents using modern AI prediction technologies.

MATERIALS AND METHODS

Ziziphus Green Extraction

Plant material preparation: *The* dried *Ziziphus spina-Christi* fruits purchased from the local market in Ramadi City/ Iraq, were ground to a powder using a high-speed multi-functional electric crusher (600W, 20000r/m, Germany). The ground fruits were sieved to isolate the

kernels. The jujube powder was ground again to make it smoother and then subjected to green extraction.

Plant Extraction: Two green extraction methods were utilized to extract as much as possible of the phenolic compounds content in Ziziphus spina-Christi (Sidr). The supercritical CO_2 extraction method of Song *et al.*, was employed with some modifications. The Sidr powder (1500g) was subjected to the supercritical CO_2 extractor (Supercritical CO_2, Green Extraction, Spe-ed TM SFE-2/4 system, Applied Separation, USA) with 95% ethanol as a co-solvent. The extraction conditions were as follows: dynamic extraction time: 2 hours; static time: 1.5 hours; CO_2 flow rate: 55g/min; CO_2 pressure: 300 bar; vessel (oven) temperature: 50°C and collection valve temperature: 120°C. Co-solvent was evaporated using a rotary evaporator ((BÜCHI Labortechnik AG, Flawil, Switzerland) [23]. The defatted residues were further extracted with 65% ethanol using ultrasonic assisted technique (700 W output with 18 kHz converter (Sonics, USA) for 1 minute at room temperature. Then the extract was filtrated with a cotton cloth followed by Whatman No.1 filter paper. Alcohol was evaporated using a rotary evaporator (BÜCHI Labortechnik AG, Flawil, Switzerland), and the rest residues were freeze-dried (Labconco cooperation, Kansas City, USA) at −53°C for 48h under 0.1 mBar, then milled and kept at −8 °C in tight plastic bags in a cool and dark place until further analysis [24].

Phenolic compounds analysis with HPLC: An Agilent 1260 series was used for the HPLC analysis. 4.6 mm x 250 mm i.d., 5 m, Eclipse C18 column was used for the separation. Water (A) and 0.05% trifluoroacetic acid in acetonitrile (B) were the components of the mobile phase, which had a flow rate of 1 ml/min. The linear gradient was sequentially programmed into the mobile

phase as follows: 12–15 minutes (82% A), 15–16 minutes (82% A), and 16–20 minutes (82% A) are all within the acceptable range. At 280 nm, the multi-wavelength detector was observed. The sample solutions were injected in a 5µl volume. The column was kept at a constant temperature of 40 °C. A standard curve quantification was employed using the phenolic compounds' standard solutions [25].

Molecular Docking

Protein preparation: The X-ray structure of the selected proteins was downloaded from the Protein Data Bank (PDB) website (https://www.rcsb.org/) in the 3D structure .pdb format. Different proteins for various therapeutic activities were selected. 3C proteinase (PDB: 1HAV) structure for anti-hepatitis A virus, X-interacting protein (PDB: 3MSH) for anti-hepatitis B virus, DNA gyrase subunit B (PDB: 6F86) for anti-*Escherichia coli* O157:H7, tyrosyl-tRNA synthetases (PDB: 1JIJ) for anti-*Staphylococcus aureus*, UDP-N-acetylenolpyruvoylglucosamine reductase (PDB: 3I99) for anti- *Vibrio cholera*, shikimate kinase (PDB: 3N2E) and urease (PDB: 1E9Y) for anti-*Helicobacter pylori*, Human topoisomerase Ⅱ beta (PDB: 3QX23) for anti-cancer activities. Proteins were directly submitted to the blind docking webserver CB-DOCK2 which removes water and hetatoms, detects the pockets available, and chooses the best one for the docking process [26]. Controls for each protein were as follows 1HAV (Amantadine) [27], 3MSH (Adefovir diphosphate) [28], 6F86 (Ciprofloxacin) [29], 1JIJ (SB239629) [30], 3I99 (Flavin Adenine Dinucleotide) (https://www.rcsb.org/structure/3I99), 3N2E ((OSA) or NSC162535) [31], 1E9Y (Acetohydroxamic acid) [32], 3QX3 (Etoposide) [33].

Preparation of the chemical compound: The detected phenolic molecules were retrieved from the PubChem website in 3D .sdf format, and then submitted directly to the CB-DOCK2 server [26].

Computational analyses: For the in-silico molecular docking assay, the previously HPLC-detected chemical compounds have been during subsequent tests. The Molecular Docking service website named "CB-Dock-2" was utilized to predict the modes of action of detected compounds from *Ziziphus spina-Christi* extracts antiviral, antibacterial, and anticancer agents. The procedure of Miraz and his co-workers was followed with modifications as necessary.[34] Bioavailability and toxicity ADMET analysis was conducted using SwissADME (http://www.swissadme.ch/) and ProTox- Ⅱ (https://tox-new.charite.de/protox_II/) web servers.

RESULTS AND DISCUSSION

Extraction and HPLC results: The supercritical CO_2-liquid extract yield was 41 ml (43g), and the ultrasonic-assisted extract powder yield was 360.13 g. The phenolic compounds of ultrasonic-assisted hydroethanolic extract and the supercritical CO_2 extract are illustrated in Table 1, and their chromatograms are shown in Figure 1 and Figure 2, respectively. The ultrasonic-assisted powder extract of jujube had five different phenolic compounds named Gallic acid (242.84 µg/g), Caffeic acid (9.75 µg/ml), Pyrocatechol (19.63 µg/g), Coumaric acid (11.92 µg/g) and Ferulic acid (16.16 µg/g), while the supercritical CO_2- liquid extract included only four phenolics named Gallic acid (108.9 µg/ml), Caffeic acid (92.1 µg/ml), Quercetin (40.7 µg/ml) and Cinnamic acid (3.69 µg/ml). Notably, the highest concentration of the detected phenolic compounds was of Gallic acid (about 351.74 µg/g total) and caffeic acid (about 101.85 µg/g). Ghafoor and her co-workers found that Rutin (15.88 mg/100g) was the primary phenolic compound in Ziziphus methanolic extract in addition to less content of Ferulic acid, chlorogenic acid, and p-hydroxybenzoic acid [35].
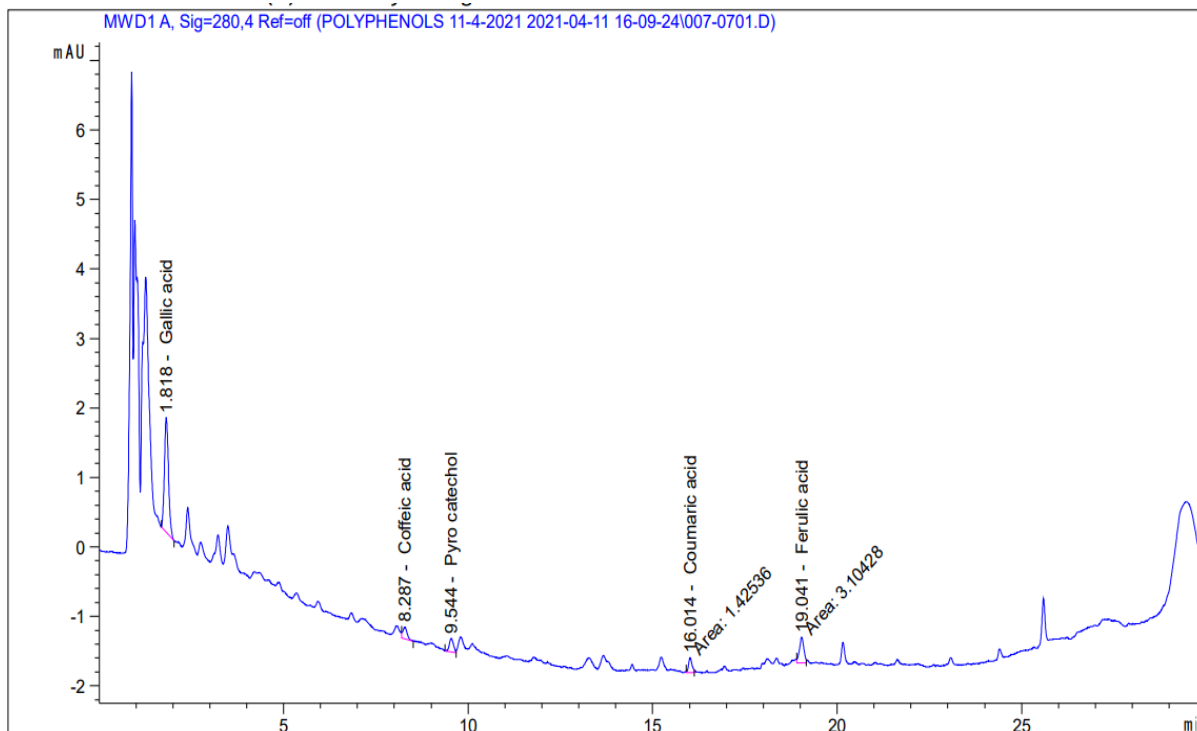
Figure 1. HPLC chromatogram of the phenolic compounds in the ultrasonic-assisted hydroalcoholic extract.
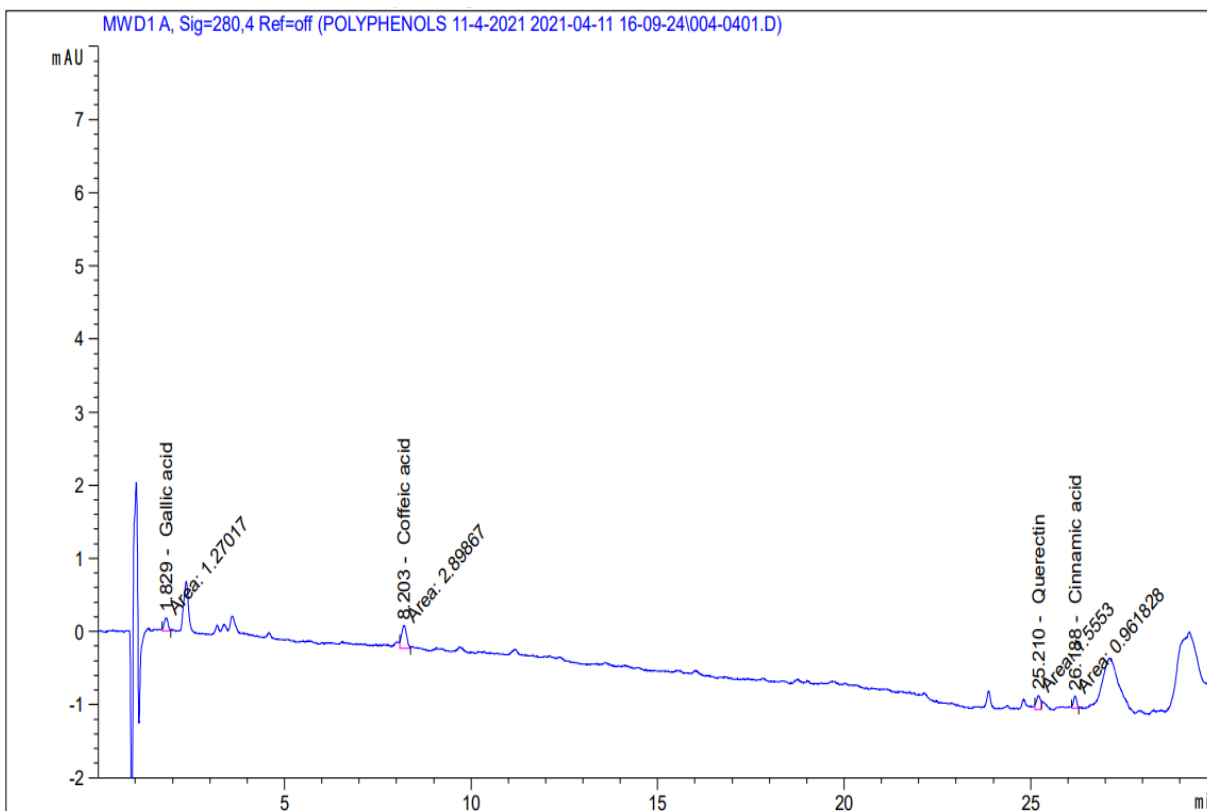
Figure 2. HPLC chromatogram of the phenolic compounds in the supercritical CO_2 extract.

Table 1. The phenolic compounds detected in the ultrasonic-assisted extract and supercritical CO_2 extract of *Ziziphus spina-Christi*

Derivative/ Compound	Area	Concentration (µg/ml=µg/22.5mg)	Conc.(µg/g)
Ultrasound-assisted extract			
Gallic acid	12.75	5.46	242.84
Chlorogenic acid	ND	ND	ND
Catechin	ND	ND	ND
Methyl gallate	ND	ND	ND
Coffeic acid	1.38	0.22	9.75
Syringic acid	ND	ND	ND
Pyro catechol	1.44	0.44	19.63
Rutin	ND	ND	ND
Ellagic acid	ND	ND	ND
Coumaric acid	1.43	0.27	11.92
Vanillin	ND	ND	ND
Ferulic acid	3.10	0.36	16.16
Naringenin	ND	ND	ND
Quercetin	ND	ND	ND
Cinnamic acid	ND	ND	ND
Kaempferol	ND	ND	ND
Hesperetin	ND	ND	ND
Supercritical CO_2-extract			
Gallic acid	1.27	10.89	108.9
Chlorogenic acid	ND	ND	ND
Catechin	ND	ND	ND
Methyl gallate	ND	ND	ND
Coffeic acid	2.90	9.21	92.1
Syringic acid	ND	ND	ND
Pyro catechol	ND	ND	ND
Rutin	ND	ND	ND
Ellagic acid	ND	ND	ND
Coumaric acid	ND	ND	ND
Vanillin	ND	ND	ND
Ferulic acid	ND	ND	ND
Naringenin	ND	ND	ND
Quercetin	1.56	4.07	40.7
Cinnamic acid	0.96	3.69	3.69
Kaempferol	ND	ND	ND
Hesperetin	ND	ND	ND

ND=not detected

Molecular docking results: The CB-Dock2-assisted blind molecular docking revealed an excellent affinity between the detected phenolic compounds and the targeted proteins (Table 2). Quercetin showed a better binding affinity with most examiner proteins than their standard ligands (Figures 3 to 10), with good Vina scores. These scores were -7.4 and -6.5 for 1HAV and 3MSH as anti-hepatitis virus A and B effects, respectively. The antibacterial activity revealed Quercetin-protein complex binding scores of -6.9, -9.9, and -9.4 for 6F86 (*E. coli*), 1JIJ (*S. aureus*), and 3I99 (*V. cholera*), respectively. For *H. pylori* inhibitory activity, Similar Vina scores (-8.5) were obtained for Quercetin docking with each of the two examined proteins, 3N2E and 1E9Y, while the anticancer activity showed an excellent Vina score with 3QX3 (-9.3).

Table 2. Molecular docking analysis for Ziziphus spina-Christi phenolic compound

Binding Vina Score									
Compound	PubChem CID	HAV (1HAV)	HBV(3 MSH)	*E. coli* DNA gyrase B (6F86)	*S. aureus* tyrosyl-tRNA synthetase (1JIJ)	*V. cholera*(3I99)	*H. pylori* shikimate kinase (3N2E)	*H. pylori* Urase (1E9Y)	Human topoisomera se II beta (3QX3)
Gallic acid	370	-5.4	-4.8	-6.1	-7.3	-6.6	-6.0	-6.0	-6.2
Caffeic acid	689043	-5.7	-5.2	-6.7	-7.1	-7.1	-6.4	-6.7	-6.5
Pyrocatechol	289	-4.8	-4.3	-5	-5.9	-5.0	-5.2	-5.1	-5.6
Coumaric acid	5280841	-5.5	-4.6	-4.9	-6.7	-5.9	-6.6	-5.7	-5.8
Ferulic acid	445858	-5.6	-5.1	-6.1	-6.9	-7.0	-6.4	-6.4	-6.4
Quercetin	5280343	-7.4	-6.5	-6.9	-9.9	-9.4	-8.5	-8.5	-9.3
Cinnamic acid	444539	-5.1	-4.8	-5.7	-6.2	-6.3	-6.3	-6.2	-5.9
Standards*		-4.9	-5.2	-5.8	-8.3	-10.1	-9.8	-3.7	-10.2

*Standards: 1HAV: Amantadine, 3MSH: Adefovir diphosphate, 6F86: Ciprofloxacin, 1JIJ: SB-239629, 3I99: Flavin-Adenine Dinucleotide, 3N2E: (OSA) NSC-162535, 1E9Y: Acetohydroxamic acid, 3QX3: Etoposide.

The Quercetin molecule showed the highest docking results with all of the tested proteins. The binding interactions with each protein were as follows:

HAV (1HAV): The best fitting pocket of hepatitis A virus 3C proteinase consists of two chains, chain A: VAL18, TRP27, VAL28, MET29, HIS44, ALA45, TYR46, PHE48, GLU49, LYS50, ASN124, HIS145, LYS146, LYS147, ASN148, PRO169, GLY170 and CYS172 and chain B: LYS106. The cavity volume was 6508 Å³, the center of the pocket was 10, 9, 10, and Docking size was 30, 33, 31. The binding interactions between 1HAV and quercetin were 2 H-bonds with GLU49, one H-bonds with each of ALA45, PHE48, HIS 44, and LYS 106, one weak H-bond with each of VAL28, GLY170, HIS44, and HIS145, one hydrophobic contact with each of VAL28 and LYS147 (Figure 3).
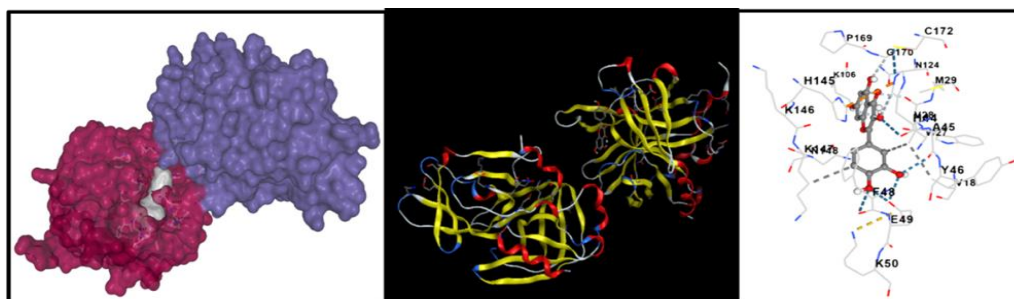
Figure 3. Quercetin-1HAV interactions.

HBV (3MSH): The best fitting pocket of hepatitis B virus X-interacting protein (3MSH) consists of one chain, including LEU5, HIS8, THR12, ILE18, VAL64, MET75, ILE76, GLN77, HIS79, ILE82, VAL84, ALA85 and VAL86, amino acids. The cavity volume was 138 $Å^3$, the center of the pocket was 0, 11, 0, and the docking size was 21, 21, 21.

The binding interactions between quercetin and 3MSH were two H-bonds with THR12, and one with each of GLN77, MET75, and VAL84, weak-H-bond with GLN77 and one hydrophobic contact with each of VAL86 and HIS79, and two with VAL84 (Figure 4).
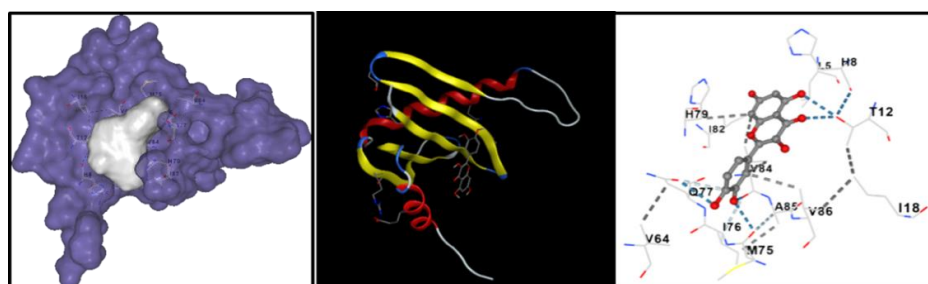
Figure 4. Quercetin- HBV (3MSH) interaction

E. coli gyrase B (6F86): The best fitting pocket of *Escherichia coli* O157:H7 DNA gyrase subunit B (6F86) consists of one chain containing: ASN46, ALA47, ASP49, GLU50, ASP73, GLY75, ARG76, GLY77, ILE78, ILE94, VAL120, GLY164 and THR165 amino acids. The cavity volume was 166 $Å^3$, the center of the pocket was 63, 30, 62, and the docking size was 21, 21, 21. The

binding interactions between quercetin and 6F86 were two H-bonds with each of ASP73, GLY77, one H-bond with each of THR165, GLU50, and ASN46, one weak-H-bond with GLU50 and one hydrophobic contact ILE94 (Figure 5).
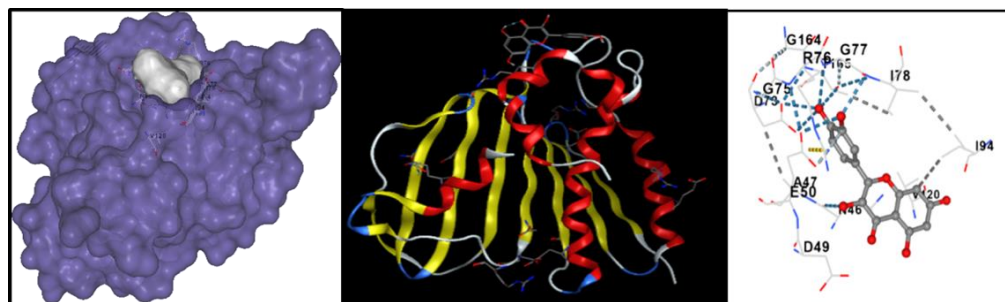
Figure 5. Quercetin- 6F86 interaction

Staphylococcus aureus Ligase (1JIJ): The best fitting pocket of *Staphylococcus aureus* tyrosyl-tRNA synthetases (1JIJ) consists of one chain of amino acids including: TYR36, CYS37, GLY38, ALA39, ASP40, THR42, HIS50, LEU70, THR75, ASP80, SER82, LYS84, ARG88, ASN124, TYR170, LEU173, GLN174, ASP177, GLN190, VAL191, ASP195, GLN196 and ILE200. The cavity volume was 2079Å^3, the center of the pocket was -14, 18, 83, and docking size was 21, 21, 21. The binding interactions between quercetin and 1JIJ were H-bonds with ASP195, LYS84, THR75, ASP177, TYR36, GLN190, weak-H-bond with GLY38, hydrophobic contacts with GLN174 (Figure 6).
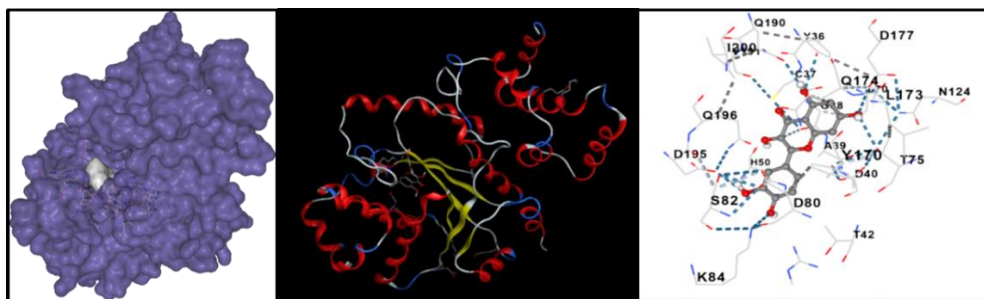
Figure 6. Quercetin- 1JIJ interactions

MurB or UDP-N acetylenolpyruvoylglucosamine reductase (3I99): The best fitting pocket of MurB (3I99) consists of one chain of amino acids involving: ILE59, ILE60, GLY61, LYS62, GLY63, SER64, ASN65, GLY126, SER130, ILE133, GLN134, PHE177, LEU181, TYR182, GLN183, ALA185, VAL186, VAL187, ARG339 and GLU346. The cavity volume is 4172, the center is 37, 12, 19, and the docking size is 35, 27, 28. The binding interactions between quercetin and 3I99 were two H-bonds with SER64, one H-bond with each of VAL187, ALA 185, GLY61, and GLY63, weak-H-bond with VAL186, two hydrophobic contacts with each of IL133, and one with each of ILE59 and ASN65 (Figure 7).
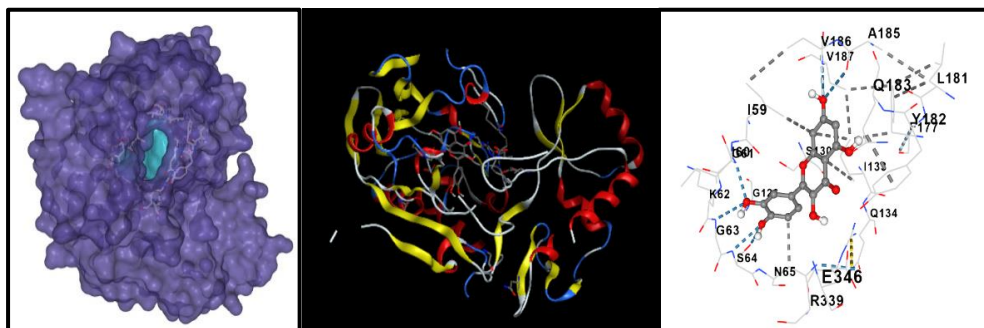
Figure 7. Quercetin- 3I99 interactions

Helicobacter pylori shikimate kinase (3N2E): The best fitting pocket of Helicobacter pylori shikimate kinase (3N2E) consists of two chains, chain A: LYS98, GLU137and ILE143, and chain B: MET10, VAL44, ARG45, GLU46, PHE48, GLU49, GLU53, LYS111, GLU112, LYS115 and ARG116. The cavity volume is 1946, the center is 59, 19, 7, and the docking size is 21, 21, 21. The binding interactions are two H-bonds with ARG45 and one hydrophobic contact with each of PHE48, LYS115, and ILE143 (Figure 8).
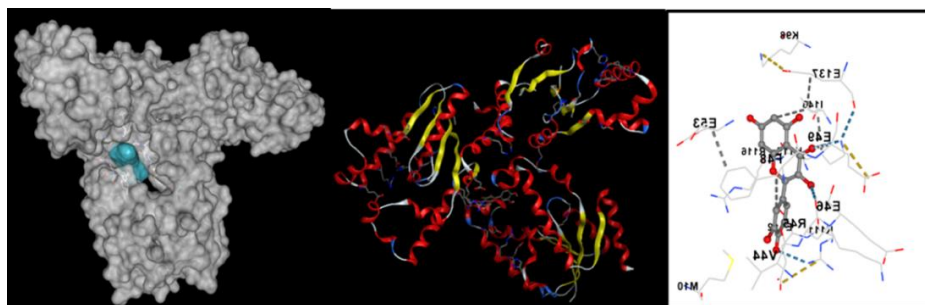
Figure 8. Quercetin-3N2E interactions

***Helicobacter pylori* urease (1e9y):** The best fitting pocket of Helicobacter pylori urease (1E9Y) consists of two chains, chain A: TYR32 VAL33 and chain B: SER438 PHE441 LYS445 PRO446 ASN447 GLN459 GLN471 VAL473 TYR474 TYR475 ILE568. The cavity volume is 2893, the center is 141, 108, 59, and the docking size was 27,31,21.

The binding interaction between quercetin and 1E9Y were to H-bonds with TYR32, one H-bond with each of VAL473, GLN459, ASN447, LYS445, one weak H-bond with VAL473, one cation-pi interaction LYS445, one pi-pi staking PHE441 and one hydrophobic contact with LYS445 (Figure 9).
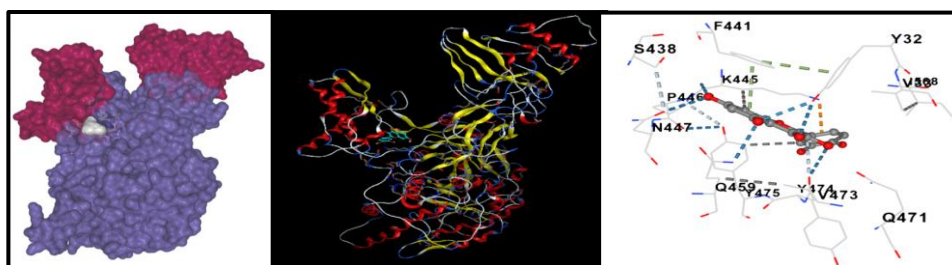
Figure 9. Quercetin-1e9y interactions

Human topoisomerase* Ⅱ *beta (3QX3): The best fitting pocket of Human topoisomerase Ⅱ beta 3QX23 consists of one chain including LYS456, GLY478, ASP479, PRO501, LEU502, ARG503, GLY504, and MET782 amino acids. the cavity volume was 33184 Å3, the center was 31, 105, 45,

and docking size was 35, 35, 35. The binding interactions between quercetin and 3QX3 were three weak-H-bonds and two H-bonds each of, HET12, two weak-H-bonds and two H-bonds with HET13 and one H-bond with HET9, three H-bonds with ASP479, two hydrophobic contacts with ATRG503 and pi-pi staking with HET12 (Figure 10).
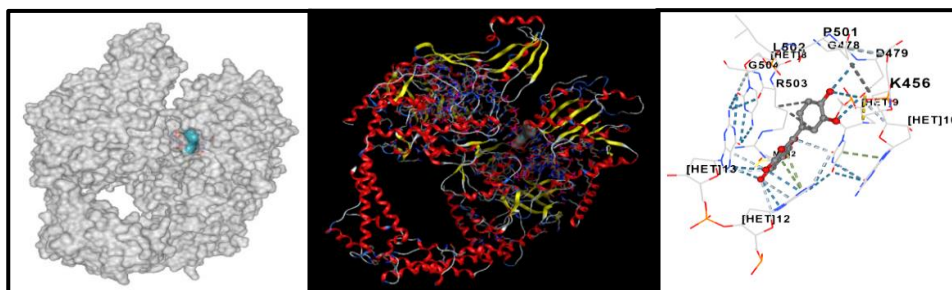
Figure 10. Quercetin-3QX3 interactions

ADMET analysis: The bioavailability ADME and toxicity analysis examination of the detected phenolic compound quercetin are shown in Table 3. Quercetin obeyed Egan

and Lipinski's rule of five and had low toxicity within limits. It is water soluble and bioavailable, and the BOILED-Egg model of the n-octanal/water partitioning

coefficient reveals good absorption in the gastrointestinal tract and no crossing for the brain-blood barrier BBB (Figure 11).

Molecular Dynamics: The 2D and 3D interactions between Quercetin and the proteins which gave the highest Vina scores are shown in Figure 12.

Table 3. ADMET analysis for quercetin.

Feature	Test	Parameter	Degree	Result
Drug likeliness	Lipinski's rule of five	Molecular weight	302.24 g/mol	Yes: 0 violation
		H-Donor	5	
		H-Acceptor	7	
		Log$P$	-0.56	
	Bioavailability score			0.55
	Egan			Yes
Pharmacokinetics	GI absorption			High
	BBB			No
	Octanol/water partition coefficient		1.99	
Water solubility				Soluble
Toxicity	Hepatotoxicity			Inactive
	Cytotoxicity			Inactive
	Immunotoxicity			Inactive
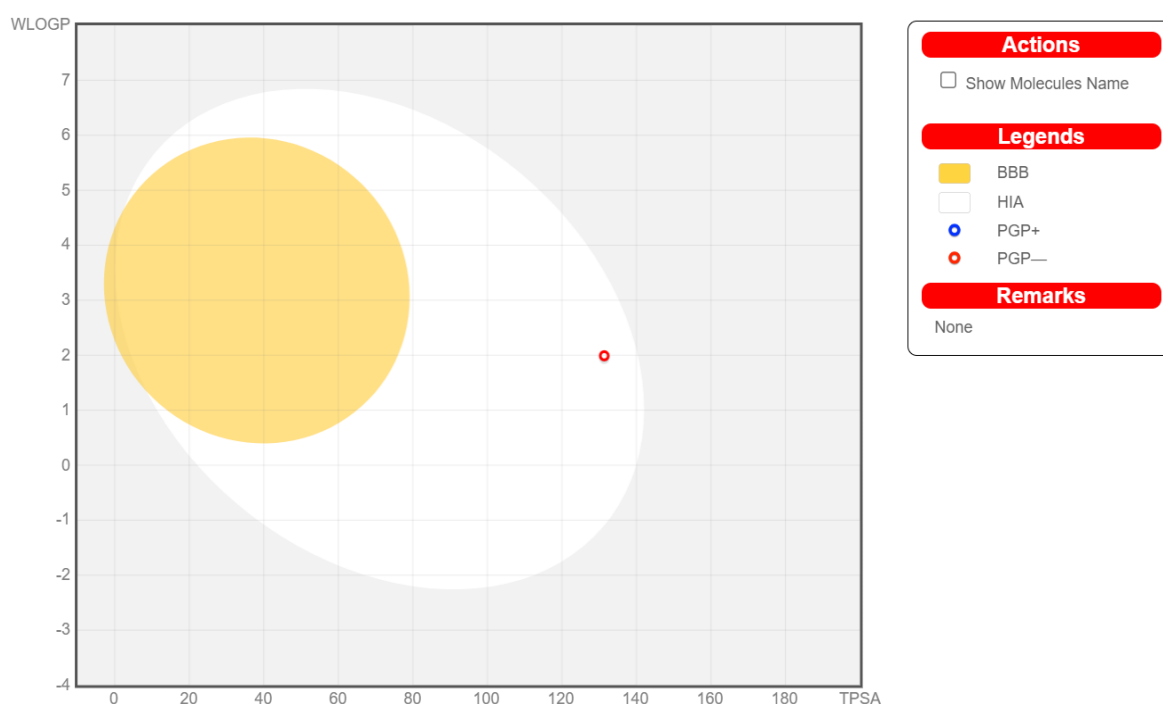
Figure 11. BOILED-Egg bioavailability model of quercetin.
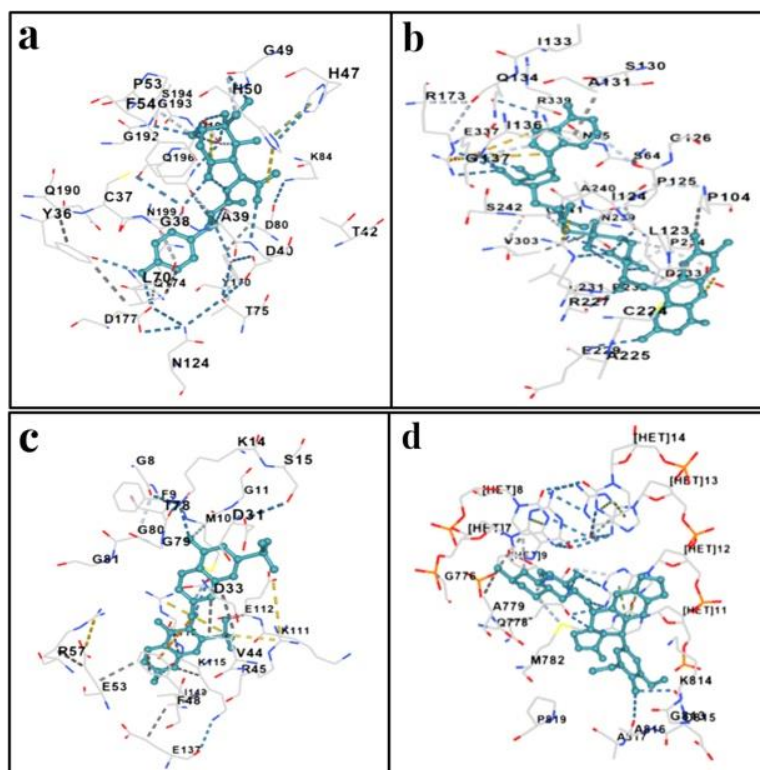
Figure 12. Standard ligands-Protein 3D docking model for each of (a): SB-239629-1JIJ, (b): FAD-3I99, (c): OSA(NSC162535)-3N2E, and (d): Etoposide-3QX3.

The RMSD studies of the protein (PDB ID 1JIJ) are shown in (Figure 13) for the entire simulation of 100ns. The study reveals that the standard (SB-239629) and test compound (Quercetin) exhibit similar stability profiles with deviation values below the threshold of 0.3 nm. Additionally, the RMSD graph of the ligand (Figure 14) shows the highest stability of the Quercetin with a minor deviation within the threshold range of 0.05 nm during the entire simulation. When compared with the ranges of deviation, the stability of the protein when complexed with Quercetin is better than the standard complex, suggesting it might have potential binding affinities with the protein structure.
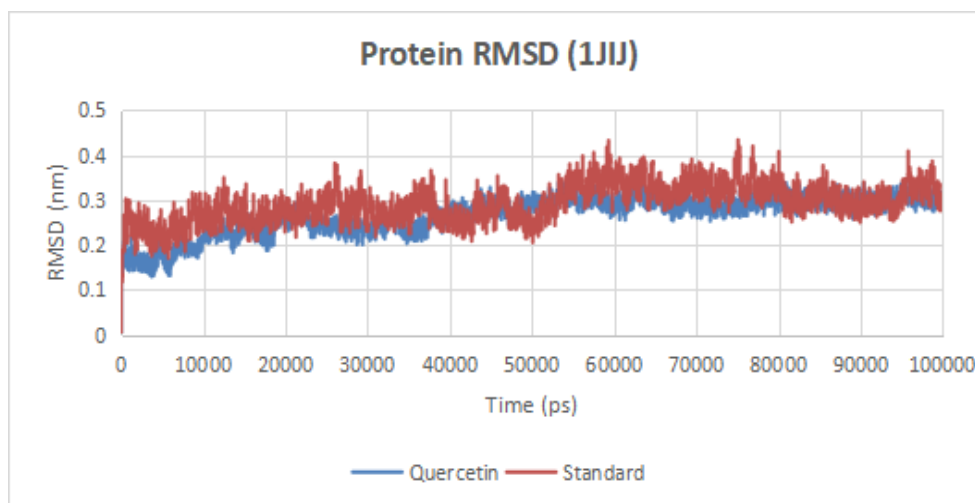
Figure 13. Protein RMSD of standard (SB-239629) and test compound (quercetin)
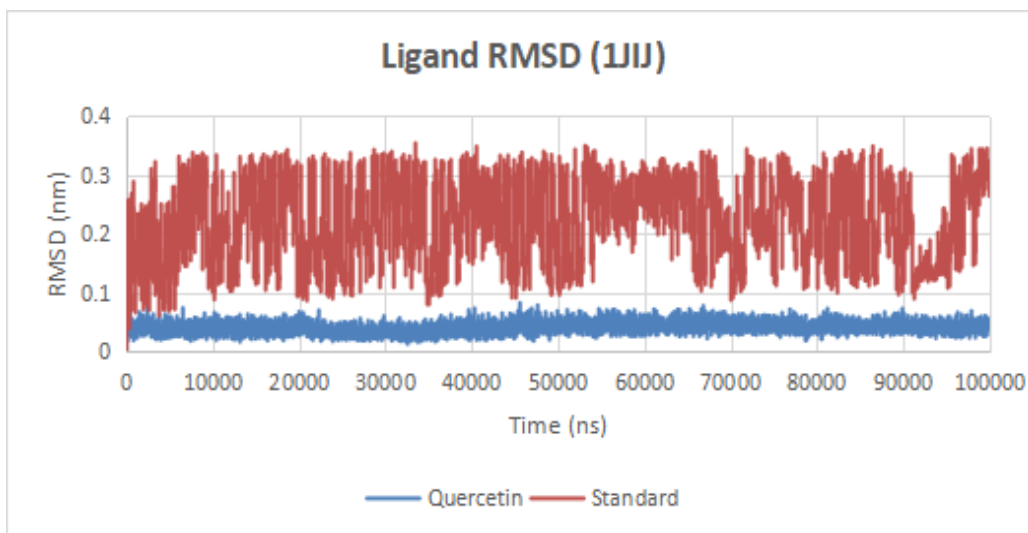
Figure 14. Ligand RMSD of standard (SB-239629) and test compound (quercetin)

The RMSF graph in Figure 15 exhibits the minimal fluctuation of the protein residues when the Quercetin is bound to the protein. Higher fluctuations were not observed throughout the simulations and were highly comparable with the standard drug. Similar patterns between the test and standard showcase strong evidence for the potential binding of the test compound without showing any strong residual fluctuation in the binding site.
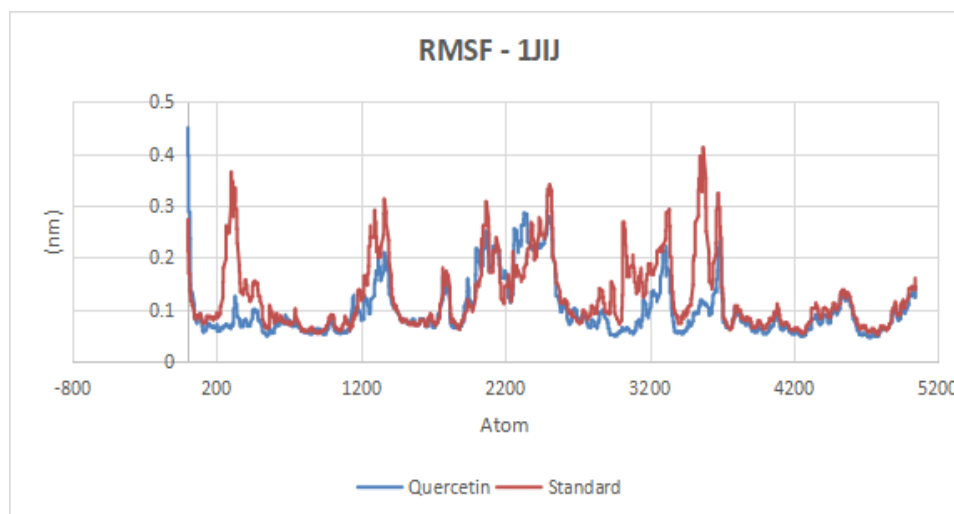
Figure 15. RMSF of standard (SB-239629) and test compound (quercetin).

A molecular dynamics study was reported in an aqueous solution. The Root-Mean-Square Deviation (RMSD) graph obtained from the molecular dynamic simulations revealed that the UDP-N-acetylenolpyruvoylglucosamine reductase (3I99) protein did not show stability with the test compound over the simulation time of 100ns. The RMSD values are in the threshold range of 1.5 to 5 nm, indicating that the protein has experienced a maximal structural deviation from its initial conformation. Compared with the RMSD of the standard drug, Quercetin tends to attain its minimal deviation around 90ns. Standard complex attained its maximal deviation at 50ns and continued to increase its deviation till 100ns. The standard complex displayed RMSD values starting

from 1.5nm to 5nm, whereas the Quercetin complex showed its initial RMSD value from 1.5nm but attained its stability with 2.0nm by the end of 100ns. This indicates

that when compared with standard, Quercetin is a suitable binder for the 3I99 protein for stabilization. (Figure 16)
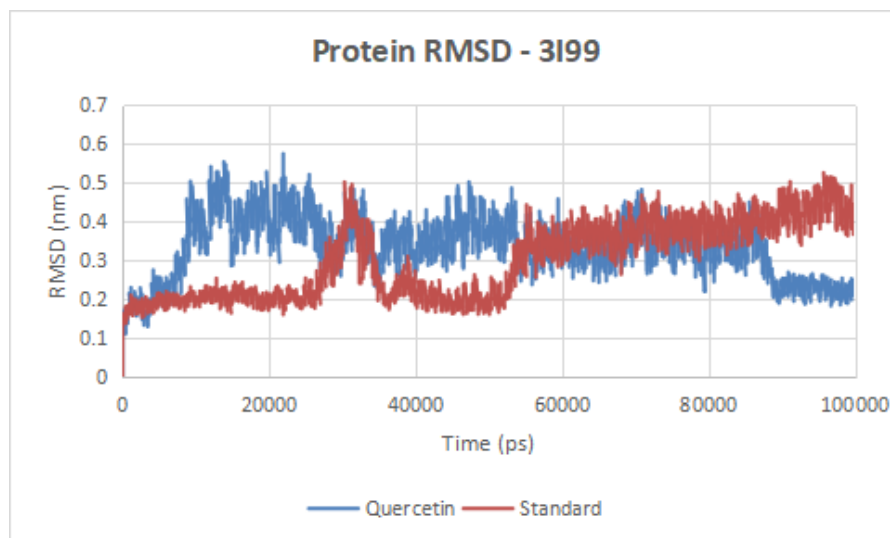
Figure 16. Protein RMSD of standard (FLAVIN-ADENINE DINUCLEOTIDE) and test compound (quercetin)

The RMSD analysis of the ligands suggests that test compound quercetin has experienced minor deviations, which might have led to pose correction in the simulation throughout 100ns. The standard molecule has maximal fluctuations observed, where the RMSD values exceeded 2nm during the initial stage and attained stability at 4nm later.

Quercetin RMSD value was approximately 0.5nm to 1.3nm. The observed fluctuations in certain regions indicate the possible orientations of the ligand within the protein binding site to attain a single stable conformation with Quercetin. So, when considering Ligand RMSD, Quercetin is way more compatible with the 3i99 protein than the standard molecule. (Figure 17)
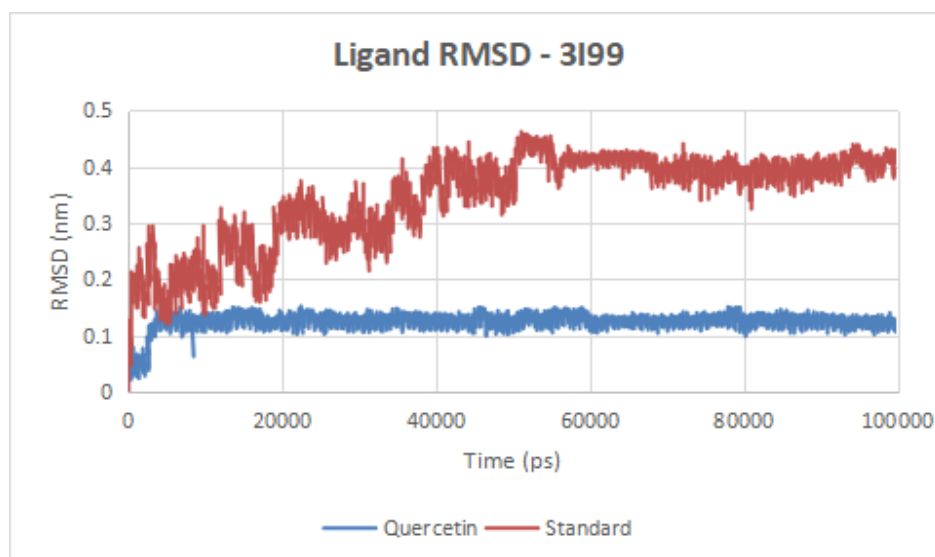
Figure 17. Ligand RMSD of standard (FLAVIN-ADENINE DINUCLEOTIDE) and test compound (quercetin)

In addition to analyzing RMSD, we further examined the Root-Mean-Square Fluctuation (RMSF) profiles. RMSF studies for both standard and test compound quercetin demonstrated similar patterns, with high fluctuations

observed at 2700 to 3000 and between 3600 to 4000 atoms within the protein (Figure 18).

Protein RMSF - 3i99
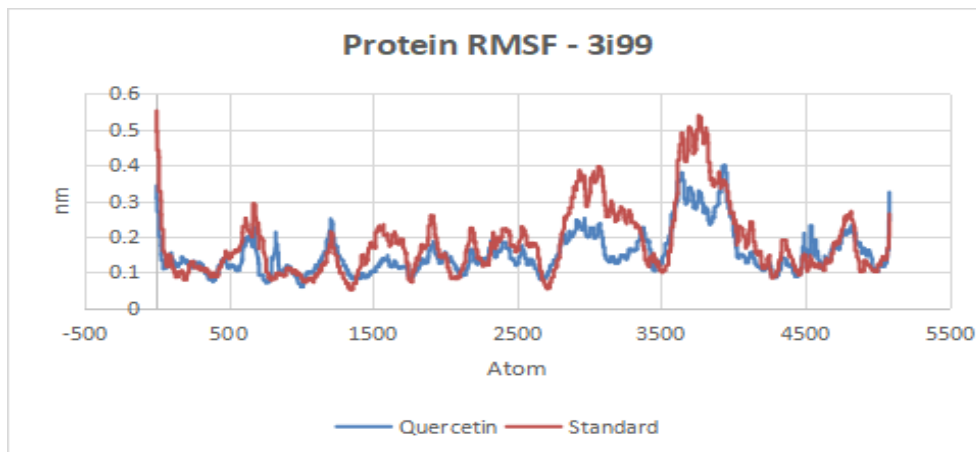
Figure 18. RMSF of standard (Flavin-Adenine Dinucleotide) and test compound (quercetin)

The RMSD studies of the protein (PDB ID 3QX3) are plotted in Figure 19 for the entire simulation of 100ns. The study reveals that standard (Etoposide) and Quercetin show a high RMSD range of 0.6-0.7 nm. Even though the initial deviations are high for quercetin before 50ns, it converges after 50ns with minimal difference in the deviation values. Since the RMSD of the protein with Quercetin is highly comparable with the known standard complex, it can be considered a suitable binder. The close

Resemblance between the structure bound to Quercetin and the standard complex demonstrates the potential affinity of Quercetin towards the protein despite the higher range of RMSD.

Additionally, the RMSD graph of the ligand (Figure 20) shows the deviation within the range of 0.1-0.2 nm. However, the values are acceptable as they exhibit a minimal deviation between the standard and Quercetin.
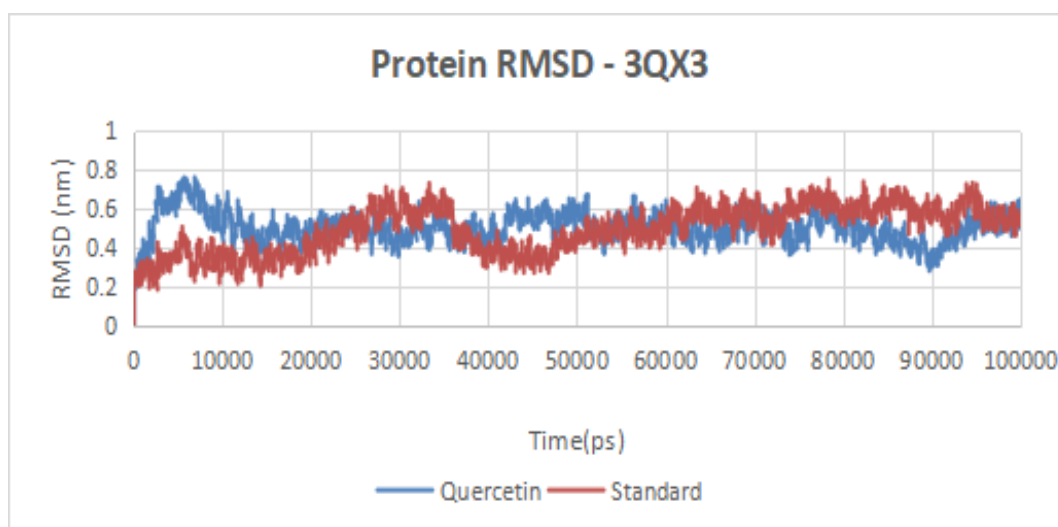
Protein RMSD - 3QX3

Figure 19. Protein RMSD of standard (Etoposide) and test compound (quercetin).
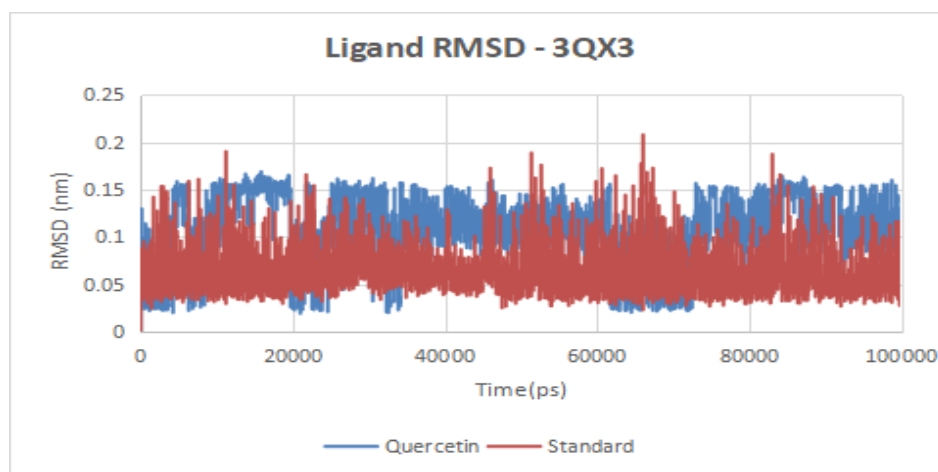
Figure 20. Ligand RMSD of standard (Etoposide) and test compound (quercetin).

The RMSF graph in Fig 3 exhibits the minimal fluctuation of the protein residues when the Quercetin is bound to the protein. Higher fluctuations were not observed throughout the simulations and were highly comparable with the standard drug (Etoposide). Similar patterns between the test and standard showcase strong evidence for the potential binding of the test compound without showing any strong residual fluctuation in the binding site. (Figure 21)
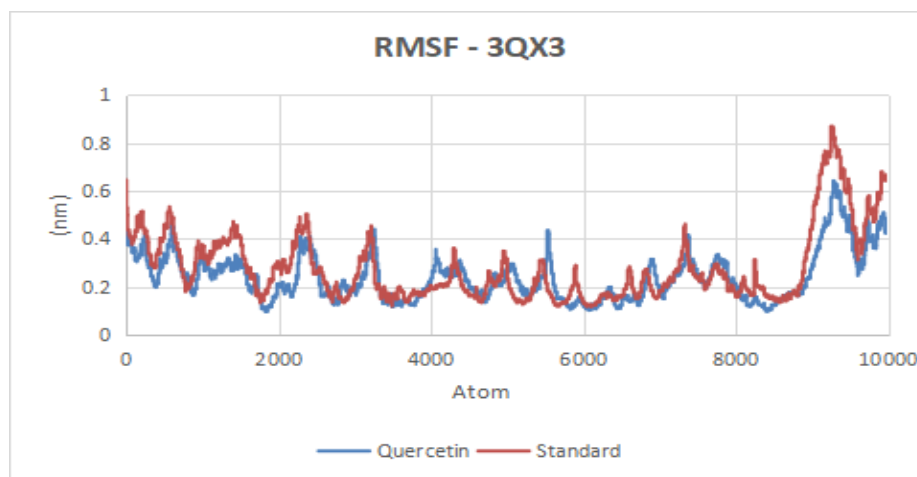
Figure 21. RMSF of standard (Etoposide) and test compound (quercetin)

The RMSD studies of the protein (PDB ID 3N2E) are shown in Figure 22 for the entire simulation of 100ns. The study reveals that the standard (NSC-162535) and test compound exhibit similar stability profiles with the deviation value ranging below the threshold of 0.25 nm. A deviation value below this threshold suggests the protein structure is relatively stable throughout the simulation for both compounds.

Additionally, the RMSD graph of the ligand (Figure 23) shows the deviation within the range of 0.2-0.25 nm. The values are acceptable despite the highest deviation between 20-60 ns as it converges to the minimal deviation after 60 ns. This suggests that quercetin could be a suitable binder.
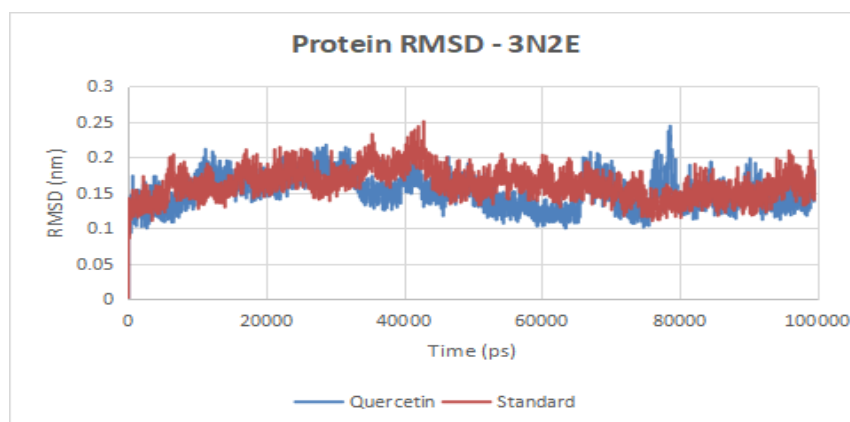
Figure 22. Protein RMSD of standard (NSC-162535) and test compound (quercetin)
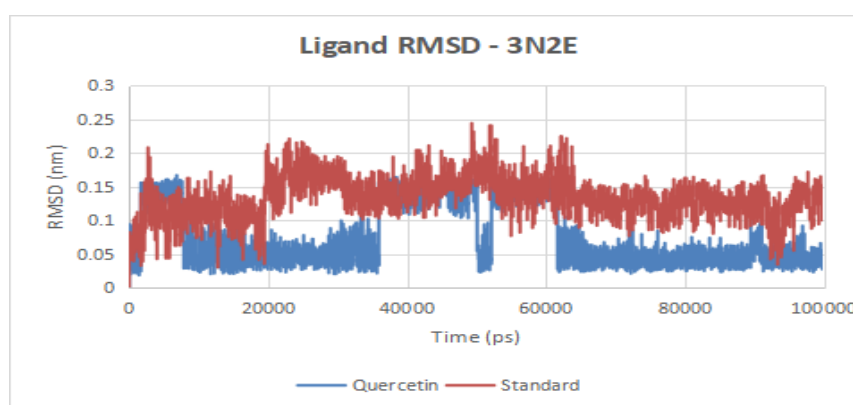
Figure 23. Ligand RMSD of standard (NSC-162535) and test compound (quercetin)

The RMSF graph in Figure 24 exhibits the minimal fluctuation of the protein residues when the Quercetin is bound to the protein. Higher fluctuations were not observed throughout the simulations and were highly comparable with the standard drug (NSC-162535).

Similar patterns between the test and standard showcase strong evidence for the potential binding of the test compound without showing any strong residual fluctuation in the binding site.
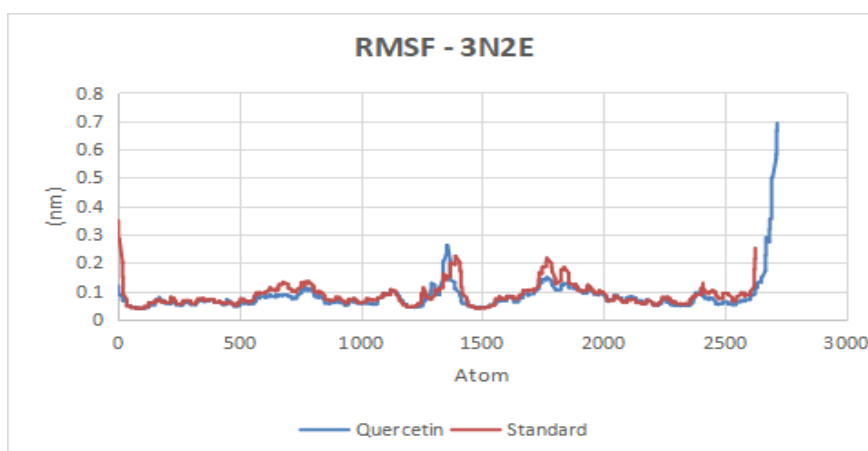
Figure 24. RMSF of standard (NSC-162535) and test compound (quercetin)

CONCLUSION

The present study aims to characterize phytochemicals extracted from Ziziphus spina-Christi (L.) Willd. for anti-viral, anti-bacterial, and anti-cancer properties by computational screening. The results obtained from molecular docking phytochemical quercetin showed good binding scores and interactions with S. aureus tyrosyl-tRNA synthetase (1JIJ), V. cholera UDP-N-acetylenolpyruvoylglucosamine reductase (3I99), Human topoisomerase Ⅱ beta (3QX3) and H. pylori shikimate kinase (3N2E). Drug likeness, bioavailability, and toxicity studies indicate that quercetin has zero violations and low toxicity parameters are within limits. Molecular dynamics studies revealed that V. cholera (3I99), Human topoisomerase Ⅱ beta (3QX3), and H. pylori shikimate kinase (3N2E) proteins do not show effective stabilities and more fluctuations were observed. Quercetin with S. aureus tyrosyl-tRNA synthetase (1JIJ) showed good stability and formed a stable complex with good RMSD and RMSF. Based on the results obtained compound Quercetin can be a potent molecule to treat bacterial infections related to the antibiotic-resistant Staphylococcus aureus. Sidr (Ziziphus spina-Christi (L.) Willd) is a widely consumed fruit globally and it has been used in traditional medicine since ancient times, so using the plant extracts may be a potent anti-bacterial treatment. These results need to be further studied in vitro and in vivo to prove its effectiveness.

AUTHORS CONTRIBUTION: Fadwa W. Abdulqahar: Conceptualization, Methodology, Validation, Formal Analysis, Interpretation of biological data, and Writing – Software Review and Editing. Zuhair I. Mahdi: Conceptualization, Methodology, Validation. Shaymaa H. M. Al-kubaisy: Formal analysis, Investigation, Software, Writing-Original draft and Visualization. Feryal F. Hussein: Writing-Reviewing and Final Editing. Kurbonova Malikakhon: Data duration, Methodology and Validation. Marwa M. El-Said: Conceptualization, Methodology, Validation, Formal analysis. Tamer M. El-Messery: Investigation, Software, Writing-Original draft, and Visualization.

REFERENCES

1. Norouzi, M., Pour, P. M., and Asgary, S. Camellia sinensis in the form of green and black tea for the primitive prophylactive effect on cardiovascular disease. Food Bioactive Compounds in Cardiovascular Diseases, 2022, 1(11), 1-3.
DOI: https://doi.org/10.31989/fbccd.v1i11.1026

2. Parvez, M. K., Rehman, M. T., Alam, P., Al-Dosari, M. S., Alqasoumi, S. I., and Alajmi, M. F.. Plant-derived antiviral drugs as novel hepatitis B virus inhibitors: Cell culture and molecular docking study. Saudi Pharmaceutical Journal, 2019, 27(3), 389-400.
DOI: https://doi.org/10.1016/j.jsps.2018.12.008

3. Abd El-Gawad, A., Kenawy, M. A., El-Messery, T. M., Hassan, M. E., El-Nekeety, A. A., and Abdel-Wahhab, M. A. Fabrication, and characterization of bee venom-loaded nanoliposomes: Enhanced anticancer activity against different human cancer cell lines via the modulation of apoptosis-related genes. Journal of Drug Delivery Science and Technology, 2023, 84, 104545.
DOI: https://doi.org/10.1016/j.jddst.2023.104545

4. Kayode, A. A., Adebodun, G. O., Fabunmi, D. I., and Kayode, O. T. Role of functional foods in the management of diabetes mellitus: a concise review. Bioactive Molecules and Pharmaceuticals, 2023, 2(7), 29-42. DOI: https://doi.org/10.31989/bmp.v2i7.1132

5. Baharoglu, Z., and Mazel, D. Vibrio cholerae triggers SOS and mutagenesis in response to a wide range of antibiotics: a route towards multiresistance. Antimicrobial agents and chemotherapy, 2011, 55(5), 2438-2441. DOI: https://doi.org/10.1128%2FAAC.01549-10

6. Bantawa, K., Sah, S. N., Subba Limbu, D., Subba, P., and Ghimire, A. Antibiotic resistance patterns of Staphylococcus aureus, Escherichia coli, Salmonella, Shigella and Vibrio isolated from chicken, pork, buffalo and goat meat in eastern Nepal. *BMC research notes*, 2019, *12*(1), 1-6. DOI: https://doi.org/10.1186/s13104-019-4798-7

7. Elrais, A. M., Arab, W. S., Sallam, K. I., Elmegid, W. A., Elgendy, F., Elmonir, W., et al. Prevalence, Virulence Genes, Phylogenetic Analysis, and Antimicrobial Resistance Profile of Helicobacter Species in Chicken Meat and Their Associated Environment at Retail Shops in Egypt. *Foods*, 2022, *11*(13), 1890. DOI: https://doi.org/10.3390/foods11131890

8. Zhang, N., Xiang, Y., Shao, Q., Wu, J., Liu, Y., Long, H. et al. Different risk and prognostic factors for liver metastasis of breast cancer patients with de novo and relapsed distant metastasis in a Chinese population. *Frontiers in Oncology*, 2023, *13*, 1102853. DOI: https://doi.org/10.3389/fonc.2023.1102853

9. Harbeck, N., Penault-Llorca, F., Cortes, J., Gnant, M., Houssami, N., Poortmans, P., et al, Breast Cancer Nat Rev Dis Primers, 2019, 5: 66. DOI: https://doi.org/10.1038/s41572-019-0111-2

10. Rizeq, B., Gupta, I., Ilesanmi, J., AlSafran, M., Rahman, M. M., and Ouhtit, A. The power of phytochemicals combination in cancer chemoprevention. *Journal of Cancer*, 2020, *11*(15), 4521. DOI: https://doi.org/10.7150%2Fjca.34374

11. Shrihastini, V., Muthuramalingam, P., Adarshan, S., Sujitha, M., Chen, J. T., Shin, H., and Ramesh, M. Plant derived bioactive compounds, their anti-cancer effects and in silico approaches as an alternative target treatment strategy for breast cancer: An updated overview. *Cancers*, 2021, *13*(24), 6222. DOI: https://doi.org/10.3390%2Fcancers13246222

12. Mtewa, A. G., Egbuna, C., Beressa, T. B., Ngwira, K. J., and Lampiao, F. Phytopharmaceuticals: Efficacy, safety, and regulation. In *Preparation of Phytopharmaceuticals for the Management of Disorders*, 2021, pp. 25-38, Academic Press. DOI: https://doi.org/10.1016/B978-0-12-820284-5.00010-1

14. Dafni, A., Levy, S., and Lev, E. The ethnobotany of Christ's Thorn Jujube (Ziziphus spina-christi) in Israel. *Journal of ethnobiology and ethnomedicine*, 2005, *1*(1), 1-11. DOI: https://doi.org/10.1186/1746-4269-1-8

15. Dkhil, M. A., Kassab, R. B., Al-Quraishy, S., Abdel-Daim, M. M., Zrieq, R., and Moneim, A. E. A. Ziziphus spina-christi (L.) leaf extract alleviates myocardial and renal dysfunction associated with sepsis in mice. *Biomedicine and Pharmacotherapy*, 2018, *102*, 64-75. DOI: https://doi.org/10.1016/j.biopha.2018.03.032

16. WebMed, Zizyphus - Uses, Side Effects, and More. [https://www.webmd.com/vitamins/ai/ingredientmono-62/ziziphus] (Retrieved on May 3rd, 2023).

17. Alsayari, A., and Wahab, S. Genus Ziziphus for the treatment of chronic inflammatory diseases. *Saudi Journal of Biological Sciences*, 2021, *28*(12), 6897-6914. DOI: https://doi.org/10.1016%2Fj.sjbs.2021.07.076

18. Zandiehvakili, G., and Khadivi, A. Identification of the promising Ziziphus spina-christi (L.) Willd. genotypes using pomological and chemical proprieties. *Food Science and Nutrition*, 2021, *9*(10), 5698-5711. DOI: https://doi.org/10.1002/fsn3.2535

19. Hassan, A. B., Al Maiman, S. A., Mohammed, M. A., Alshammari, G. M., Alkhudhayri, D. A., Alhuthayli, H. F, et al. Effect of natural fermentation on the chemical composition, mineral content, phytochemical compounds, and antioxidant activity of Ziziphus spina-christi (L.) "Nabag" seeds. *Processes*, 2021, *9*(7), 1228. DOI: https://doi.org/10.3390/pr9071228

20. Abdulqahar, F. W., El-Messery, T. M., Zaky, A. A., and El-Said, M. M. In vitro digestibility of Aucklandia costus-loaded nanophytosomes and their use in yoghurt as a food model. Food Bioscience, 2022, 50, 102106. DOI: https://doi.org/10.1016/j.fbio.2022.102106.

21. Abdel-Wahhab, M. A., El-Nekeety, A. A., Mohammed, H. E., El-Messery, T. M., Roby, M. H., Abdel-Aziem, S. H., and Hassan, N. S. Synthesis of encapsulated fish oil using whey protein isolate to prevent the oxidative damage and cytotoxicity of titanium dioxide nanoparticles in rats. Heliyon, 2021, 7(11). DOI: https://doi.org/10.1016/j.heliyon.2021.e08456

22. Bantawa, K., Sah, S. N., Subba Limbu, D., Subba, P., and Ghimire, A. Antibiotic resistance patterns of Staphylococcus aureus, Escherichia coli, Salmonella, Shigella and Vibrio isolated from chicken, pork, buffalo and goat meat in eastern Nepal. *BMC research notes*, 2019, *12*(1), 1-6.DOI: https://doi.org/10.1186/s13104-019-4798-7

23. Abdulqahar, F. W., Morgab, M. A., Hussein, F. F., Apyantseva, Y., and El-Messery, T. M. (2023). In silico analyses of bioactive compounds extracted from ziziphus jujuba using supercritical CO2 extraction: Potential anti-anxiety and anti-Alzheimer's disease. Bioactive Compounds in Health and Disease, 6(10), 215-234. DOI: https://doi.org/10.31989/bchd.v6i10.1180

24. Shaker, B., Ahmad, S., Lee, J., Jung, C., and Na, D. In silico methods and tools for drug discovery. *Computers in biology and medicine*, 2021, *137*, 104851.
DOI: https://doi.org/10.1016/j.compbiomed.2021.104851

25. Song, L., Liu, P., Yan, Y., Huang, Y., Bai, B., Hou, X., and Zhang, L. Supercritical CO2 fluid extraction of flavonoid compounds from Xinjiang jujube (Ziziphus jujuba Mill.) leaves and associated biological activities and flavonoid compositions. *Industrial Crops and Products*, 2019, *139*, 111508.
DOI: http://dx.doi.org/10.1016/j.indcrop.2019.111508

26. El-Messery, T. M., El-Said, M. M., Salama, H. H., Mohammed, D. M., and Ros, G. Bioaccessibility of encapsulated mango peel phenolic extract and its application in milk beverage. *International Journal of Dairy Science*, 2021, *16*(1), 29-40.
DOI: https://doi.org/10.3923/ijds.2021.29.40

27. Gheraibia, S., Belattar, N., and Abdel-Wahhab, M. A. HPLC analysis, antioxidant and cytotoxic activity of different extracts of Costus specious against HePG-2 cell lines. *South African Journal of Botany*, 2020, *131*, 222-228.
DOI: https://doi.org/10.1016/j.sajb.2020.02.019

28. Liu, Y., Yang, X., Gan, J., Chen, S., Xiao, Z. X., and Cao, Y. (2022). CB-Dock2: Improved protein–ligand blind docking by integrating cavity detection, docking and homologous template fitting. *Nucleic acids research*, *50*(W1), W159-W164.
DOI: https://doi.org/10.1093/nar/gkac394

29. Al-Salahi, R., Marzouk, M., and Abuelizz, H. A. Anti-HAV evaluation and molecular docking of newly synthesized 3-benzyl (phenethyl) benzo [g] quinazolines. *Bioorganic andMedicinal Chemistry Letters*, 2019, *29*(13), 1614-1619.
DOI: https://doi.org/10.1016/j.bmcl.2019.04.043

30. Singla, R. K. Mechanistic evidence to support the anti-hepatitis B viral activity of multifunctional scaffold and conformationally restricted magnolol. *National Academy Science Letters*, 2014, *37*, 45-50.
DOI: http://dx.doi.org/10.1007/s40009-013-0195-2

31. Aliye, M., Dekebo, A., Tesso, H., Abdo, T., Eswaramoorthy, R., and Melaku, Y. Molecular docking analysis and evaluation of the antibacterial and antioxidant activities of the constituents of Ocimum cufodontii. *Scientific reports*, 2021, *11*(1), 10101.
DOI: https://doi.org/10.1038/s41598-021-89557-x

32. Beg, M. A., Ansari, S., and Athar, F. (2020). Molecular docking studies of Calotropis gigantea phytoconstituents against Staphylococcus aureus tyrosyl-tRNA synthetase protein. *J Bacteriol Mycol Open Access*, *8*(3), 78-91.
DOI: http://dx.doi.org/10.15406/jbmoa.2020.08.00278

33. Gordon, S., Simithy, J., Goodwin, D. C., and Calderón, A. I. (2015). Selective Mycobacterium tuberculosis shikimate kinase inhibitors as potential antibacterials. *Perspectives in medicinal chemistry*, *7*, PMC-S13212. DOI: https://doi.org/10.4137%2FPMC.S13212

34. AA Abdel-Aal, M. A.A., M., Abdel-Aziz, S. A., Shaykoon, M. S. A., Mohamed, M. F., and Abuo-Rahma, G. E. D. A. Antibacterial and urease inhibitory activity of new piperazinyl N-4 functionalized ciprofloxacin-oxadiazoles. Journal of Modern Research, 2019, 1(1), 1-7.
DOI: https://dx.doi.org/10.21608/jmr.2019.12650.1001

35. Sharma, K. K., Singh, B., Mujwar, S., and Bisen, P. S. Molecular docking-based analysis to elucidate the DNA topoisomerase IIβ as the potential target for ganoderic acid; a natural therapeutic agent in cancer therapy. *Current computer-aided drug design*, 2020, *16*(2), 176-189. DOI: https://doi.org/10.2174/1573409915666190820144759

36. Miraz, M. M. H., Ullah, M. A., Nayem, A. A., Chakrobortty, B., Deb, S., Laskar, A., ... and Kundu, S. K. Nigelladine a among selecin-silicounds from nigella sativa exhibits propitious interaction with omicron variant of SARS-CoV-2: An in-silico study. *International Journal of Clinical Practice*, *2023*.
DOI: https://doi.org/10.1155/2023/9917306

37. Ghafoor, A. O., Qadir, H. K., and Fakhri, N. A. Analysis of phenolic compounds in extracts of Ziziphus spina-christi using RPHPLC method. *J Chem Pharm Res*, 2012, *4*(6), 3158-3163.